

Evaluation of the hydraulic behavior of the composite hydraulic structure considering a bed flume with special obstacle

Rafi M. QASIM¹, Ihsan A. ABDULHUSSEIN¹, Alya A. MOHAMMED*¹
Qusay A. MAATOOQ¹

*Corresponding author

¹Southern Technical University, Engineering Technical College, Iraq,
rafi.mohammed@stu.edu.iq, drengihssan@stu.edu.iq, alayaalrefee@stu.edu.iq*,
kusaybasrah@yahoo.com

DOI: 10.13111/2066-8201.2022.14.3.6

Received: 21 April 2022/ Accepted: 16 August 2022/ Published: September 2022

Copyright © 2022. Published by INCAS. This is an “open access” article under the CC BY-NC-ND license (<http://creativecommons.org/licenses/by-nc-nd/4.0/>)

Abstract: *The experimental simulation between the composite hydraulic structure and the found obstacles in the downstream region is a challenging process due to the energy losses and kinematic dissipation. The current work focuses on a comparative analysis of free flow conditions that exist without obstacles and submerged flow conditions that occur due to obstacles. It indicates the evaluation of hydraulic variables and geometrical variables of composite hydraulic structure for both flow conditions. In addition, it includes an investigation of the interaction among these variables. The hydraulic variables include actual discharge, flow velocity, flow cross-sectional area that crosses the gate, downstream water depth, discharge coefficient, Reynolds number and, Froude number, while the vertical distance between the weir and gate represents the geometry variable. The interference between the weir discharge and gate discharge plays a significant role in the result fluctuation and variation for both flow conditions, while the form and size of the obstacles only have a major effect on the submerged flow. For both flow conditions, the water depth is investigated; there would be a drastic increase in water depth by using obstacles in the downstream area as compared with not using the obstacles. This study adopts different obstacles in shape and size, therefore, the variation of maximum and minimum water levels related to the location will occur.*

Key Words: *bed flume, free flow, hydraulic characteristics, obstacle, submerged flow*

1. INTRODUCTION

Any combined hydraulic structure consists of two different structures that will be operated under the flow characteristics of both of them with a high operational efficiency. The main features of the composite hydraulic structure is based on the removal of both the floating material and the sedimental material simultaneously without any fluctuation in discharge quantity or/ and deficiency in control, diversion and distribution of the stream flow in river or channel. The stream flow, sometimes, suffer from shortages in supply quantity of flow due to the presence of some objects like obstacles, pier, debris material, dike, and plants in river and/ or channel. This lead to flow energy loss and flow momentum loss. So, it is very important to study the interference between the flow that passes the hydraulic structure and any special obstacle which exists at the downstream bed flume. The present work was not tackled in

previous time by any research. The noticeable effort has been achieved to investigate the flow characteristics around an abutment or dike, based on numerical simulation. The study research dealt with this field was conducted by Tingsanchali and Maheswaran [1], Michiue and Hinokidani [2], Jia and Wang [3], Muneta and Shimizu [4], Mayerle et al. [5], Ouillon and Dartus [6], Chen and Ikeda [7], and Kimura and Hosoda [8]. The above studies mentioned the major feature of the flow field immediately at abutment or a dike, such as the values of the time-averaged velocity, and they did not reveal much about the effect of dike or abutment on the downstream separation region. Jia et al. [9] and Nagata et al. [10] used a three dimensional model to simulate the hydrodynamic flow field and the sediment transport around the super dike by solving the equation of the Reynolds – averaged Navier-Stokes equation. Qasim et al. [11] investigated the influence of bed flume contraction on composite hydraulic structure discharge coefficient as compared with the discharge coefficient of composite structure when the bed flume is shown without contraction. The study comprises the investigation of the impact of several hydraulic variables on the discharge coefficient like, discharge quantity, flow velocity, Froude number, Reynolds number, and average water depth at downstream system. It was noticed that in the downstream of the system, nonlinear water surface profile exists when a contraction of the bed flume is relative to the linear water surface profile and in case of no bed flume contracture. Qasim et al. [12] studied the effect of the barrier on the hydraulic characteristics of the composite hydraulic structure. Many experimental works were conducted to estimate the influence of the location, numbers and spacing on the water depth and the level at the downstream region of the flume, composite structure discharge coefficient and discharge throughout the flume. Also, Qasim et al. [13] carried out several experimental works to investigate the influence of the obstacle on the hydraulic properties of flow which passes through the composite hydraulic structure. Here, two different configurations of obstacle are considered in the experimental study, the first configuration is the obstacle used without opening, while the second one included the rectangular opening. This work comprises a comparison between the two different types of flow; these types are: the free flow condition and the submerged flow condition. Different cases are achieved depending on the various hydraulic variables and the dimensional variables in order to assess the presence of the obstacle without or with openings. The purpose of the present research is to examine the impact of using obstacles at the downstream region to regulate water depth rise in this area and to satisfy the submerge flow state as opposed to the free flow state that occurs without obstacles. This research also shows a linkage between the hydraulic variables and the geometric variables for both free flow and submerging flow conditions.

2. FLUID MECHANICS CONSIDERATION

In this work, three different composite hydraulic devices are considered.

1-Triangular weir (V-notch) – Ellipse gate

The flow rate that passes through the composite device is equal to the Sumiton of over flow rate from weir and under flow rate from gate.

$$Q_{theor} = Q_w + Q_g \quad (1)$$

The flow – rate of the weir (V-notch) (Streeter, 1989), [14] is:

$$Q_{weir} = \frac{8}{15} \sqrt{2g} \tan \frac{\phi}{2} h_u^{5/2} \quad (2)$$

The gate flow is obtained using the continuity equation (Streeter, 1989), [14]

$$Q = V A \quad (3)$$

$$Q_{gate} = V A = \sqrt{2gH} A \quad (4)$$

The free flow is given as

$$H = d + y + h_u \quad (5)$$

For the submerged flow we have

$$Q_{act} = c_d Q_{theor} \quad (6)$$

$$Q_{act} = c_d \left[\frac{8}{15} \sqrt{2g} \tan \frac{\phi}{2} h_u^{5/2} + \sqrt{2gH} A \right] \quad (7)$$

$$H = d + y + h_u - h_d \quad (8)$$

2-Rectangular weir – Ellipse gates

The flow rate that passes through the composite device is equal to the Sumiton of over flow rate from weir and under flow rate from gate.

$$Q_{theor} = Q_w + Q_g \quad (9)$$

The flow – rate of the weir (Streeter, 1983), [14] is:

$$Q_{weir} = \frac{2}{3} \sqrt{2g} b h_u^{3/2} \quad (10)$$

To obtain the flow-rate of the gate we use the continuity equation (Streeter, 1989), [14] as follows:

$$Q = V A \quad (11)$$

$$Q_{gate} = V A = \sqrt{2gH} A \quad (12)$$

The free flow is given as:

$$H = d + y + h_u \quad (13)$$

For the submerged flow we have

$$Q_{act} = c_d Q_{theor} \quad (14)$$

$$Q_{act} = c_d \left[\frac{2}{3} \sqrt{2g} b h_u^{3/2} + \sqrt{2gH} A \right] \quad (15)$$

$$H = d + y + h_u - h_d \quad (16)$$

3- Parabolic weir – Ellipse gates

The flow rate that passes through the composite device is equal to the Sumiton of over flow rate from weir and under flow rate from gate.

$$Q_{theo} = Q_w + Q_g \quad (17)$$

To find the flow-rate of the weir (Bos, 1989) [15] we write:

$$Q_w = \frac{\pi}{2} \sqrt{fg} h_u^2 \quad (18)$$

To obtain the flow-rate of the gate we use the continuity equation [14]

$$Q_g = V A = \sqrt{2 g H} A \quad (19)$$

For the free flow

$$H = d + y + h_u \quad (20)$$

For the submerged flow

$$Q_{act} = c_d Q_{theo} \quad (21)$$

$$Q_{act} = c_d \left[\frac{\pi}{2} \sqrt{f g} h_u^2 + \sqrt{2 g H} A \right] \quad (22)$$

$$H = d + y + h_u - h_d \quad (23)$$

where H : Upstream water height, h_u : sharp crest weir head, y : Vertical distance between weir and gate, d : Water height at the gate opening, A : Flow cross sectional area that crosses the gate opening, b : Width of the rectangular weir, V : Water flow velocity through the gate; f : Focal distance, g : Gravity acceleration, Q_{theor} : *Theoretical discharge*; Q_{act} : *Actual discharge*; c_d : *discharge coefficient*; h_d is water depth at down stream.

Reynolds Number and Froude Number are calculated using the following equations [16],[17], respectively

$$R_e = \frac{V h_d}{\nu} \quad (24)$$

$$F_r = \frac{V}{\sqrt{g y}} \quad (25)$$

where: ν is water kinematic viscosity.

3. EXPERIMENTAL WORK

The experimental work was conducted in the hydraulic laboratory of Basra engineering technical college. The flume had a total length of 2m, width of 7.5cm and depth of 15cm. The flume had rectangular cross-section. Horizontal bed flume was always adopted during the experimental run (slope=0). The volume method was used to measure the actual water flow discharge while the water depth was measured by adopting a scale which was fixed at the wall of the flume. The models of combined weir-gate hydraulic structure were made from sheet wood with 5mm thickness, bevelled along all the edges at (45°) with sharp edges of thickness (1 mm) (Qasim et. al., 2018) [18]. Obstacle models were made from wood with thickness (1 cm); also the obstacles were located at a distance, equal to 40 cm from the combined hydraulic structure at downstream system. Twelve different shapes with size were adopted in the present work. The obstacles had 10cm long and 7.5cm width. Table 1 shows the selected dimensions of the rectangular, triangular and parabolic versions, made from wood.

Figure 1 shows the combinations of the shapes which are used in the current work while figure 2 shows the different shapes of obstacles that are installed at the bed flume in the downstream region. In each run, weir water head, actual discharge, flow depth at upstream and downstream were measured under the free and submerged flow conditions. In the present analysis, the triangular, rectangular, and parabolic weirs that are superimposed on ellipse form the gate were adopted.

Table 1 - The Tested Model Dimensions, Details and Shapes of weir and Ellipse Gate

Model No.	Weir Shape	h_u (cm)	y (cm)	d (cm)	H (cm)	A_g (cm ²)	A_g/BH	Y/H
1	Triangle	3	4.0	2.0	9	7.086	0.1050	0.4444
2	Triangle	2	4.0	2.0	8	7.086	0.1181	0.5000
3	Triangle	1	4.0	2.0	7	7.086	0.1350	0.5714
4	Triangle	3	4.5	1.5	9	4.907	0.0727	0.5000
5	Triangle	2	4.5	1.5	8	4.907	0.0818	0.5625
6	Triangle	1	4.5	1.5	7	4.907	0.0935	0.6429
7	Parabola	3	4.0	2.0	9	7.069	0.1047	0.4444
8	Parabola	2	4.0	2.0	8	7.069	0.1178	0.5000
9	Parabola	1	4.0	2.0	7	7.069	0.1346	0.5714
10	Parabola	3	4.5	1.5	9	4.909	0.0727	0.5000
11	Parabola	2	4.5	1.5	8	4.909	0.0818	0.5625
12	Parabola	1	4.5	1.5	7	4.909	0.0935	0.6429
13	Rectangle	4	3.0	3.0	10	7.069	0.0943	0.3000
14	Rectangle	3	3.0	3.0	9	7.069	0.1047	0.3333
15	Rectangle	2	3.0	3.0	8	7.069	0.1178	0.3750
16	Rectangle	1	3.0	3.0	7	7.069	0.1346	0.4286
17	Rectangle	3	3.5	2.5	9	4.909	0.0727	0.3889
18	Rectangle	2	3.5	2.5	8	4.909	0.0818	0.4375
19	Rectangle	1	3.5	2.5	7	4.909	0.0935	0.5000
20	Rectangle	4	3.5	2.5	10	4.909	0.0655	0.3500

The present experimental work concerns with two different cases and these cases are:

A: bed flume without obstacles at downstream region.

B: bed flume with obstacles at downstream region.

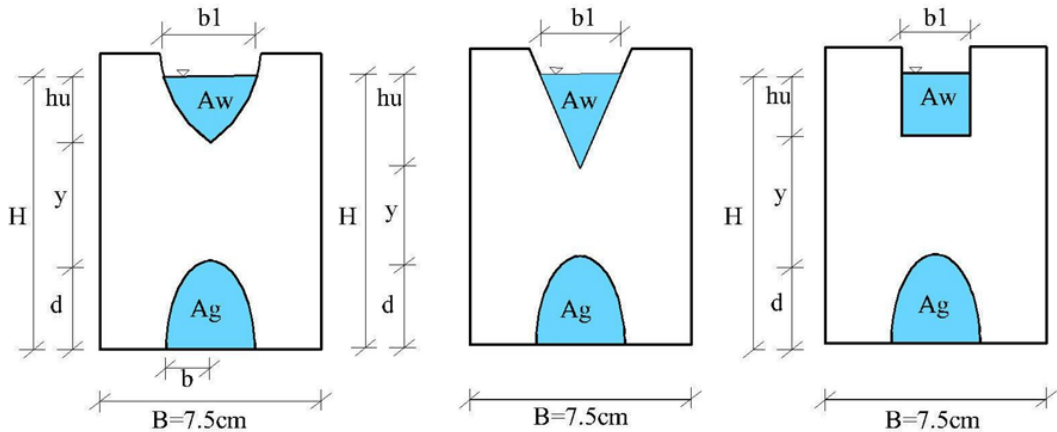


Figure 1 - Definition Sketch for the Three Models of Combined Free Flow over Weir and under Gate

4. RESULTS AND DISCUSSIONS

The designers and the hydraulic engineers who deal with the hydraulic structures found that the existence of the obstacles in rivers or open channels led to the flow losses, because of the obstacles worked as a source of flow resistance. Therefore sometimes, it is necessary to remove the obstacles or divert the flow path. In general, using of the obstacles at downstream region of any hydraulic structure leads to dissipate the water energy. The paper deals with the experimental work to investigate the effect of using the obstacles in the downstream region of the composite hydraulic structure, in order to increase the water depth and push the water as

far as possible in the downstream. Figure 3a shows the variation of the actual discharge relationship with (A_g/BH). The figure illustrates a comparative study between the free flow condition and the submerged flow condition.

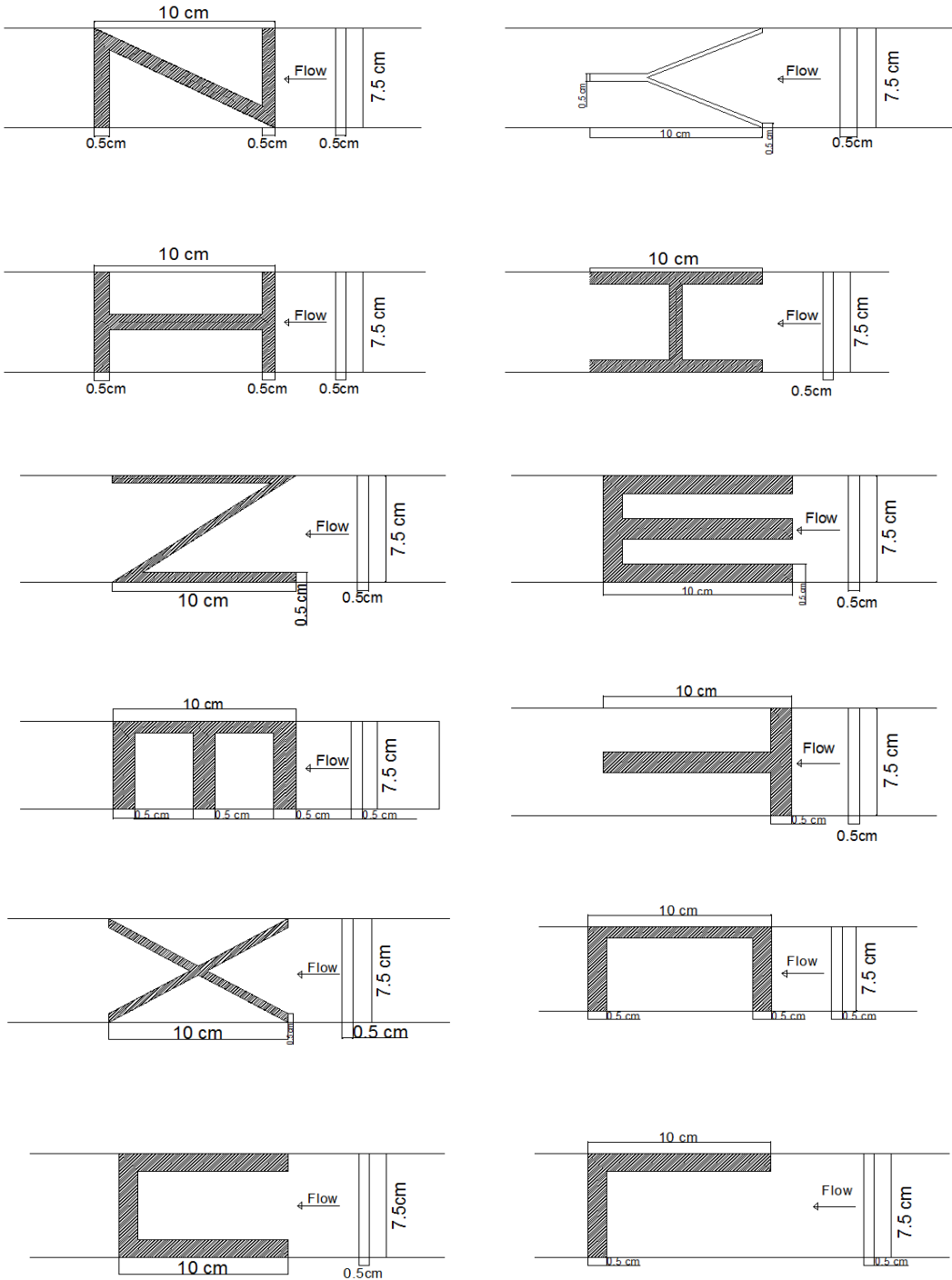


Figure 2 - The different shapes of obstacles at the downstream bed flume

From the figure given, it is clear that a complex pattern in relation between the actual discharge and (A_g/BH) is shown. For both flow conditions, the actual discharge values increase with the increasing in (A_g/BH) values. This happens because of the directly proportional relationship between the actual flow and the cross-sectional area of the flow passing through the gate A_g according to the continuity equation. In this comparison, the weir shape is limited to the rectangular, triangular and parabolic while the gate has a half ellipse shape. The submerged flow produces a maximum actual discharge as compared with the free flow. Here, the obstacle leads to the submerged flow which produces a maximum of actual discharge. The actual discharge values in free flow condition are distributed among the actual discharge values of submerged flow condition. Figure 3b shows the relationship between the discharge coefficient for the composite structure and the non-dimensional ratio (A_g/BH) . Figure 3b shows the variation of the discharge coefficient relationship with (A_g/BH) . The figure illustrates a comparative study between the free flow condition and the submerged flow condition. Figure 3b illustrates a complex pattern in the relationship between the discharge coefficient and (A_g/BH) . Here, it is very important to mention that both figures 3a, 3b have the same pattern and behavior due to the direct proportionality in the relationship between the actual discharge and the discharge coefficient.

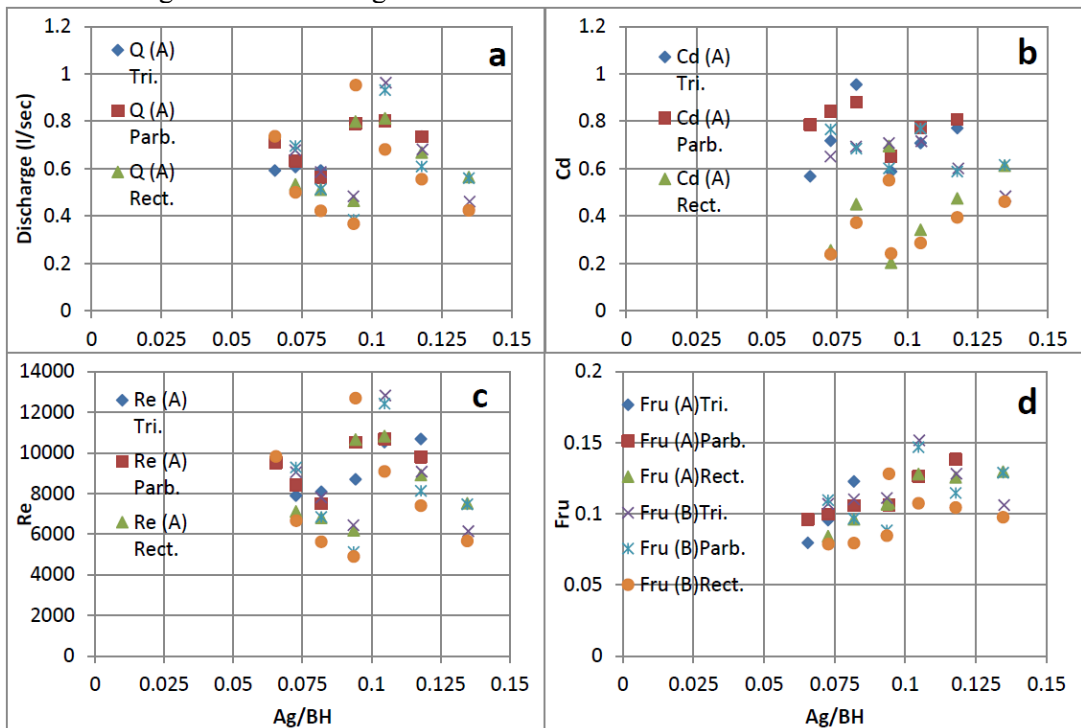


Figure 3 - Area of gate ratio with (a) Variation of Measured Discharge, (b): Variation of Discharge Coefficient, (c) Variation of Reynold's Number, (d) Variation of Upstream Froude Number

This is clear in equations (7, 15 and 22), regardless of the type of flow (free or submerged) and the presence of obstacles. It is also obvious from figure 3b, that the maximum and minimum discharge coefficient occur in free flow condition while the values of discharge coefficient in the submerged flow condition are distributed between the maximum and minimum values, respectively. The fluctuation and variation of results for both figures 3a, 3b rely on the interaction between the over flow discharge from the weir and the under flow

discharge from the gate, the obstacle shape and the dimensions that have a direct influence on the actual flow and discharge coefficient, especially in the submerged flow state.

Figure 3c illustrates the relationship between the Reynolds number and (A_g/BH) . The figure also presents a comparative study between the free flow condition and the submerged flow condition. There was a remarkable relationship between the Reynolds number and (A_g/BH) . The Reynolds number values decrease with the increasing in (A_g/BH) values. For more clarification, the Reynolds number depends on flow velocity and flow depth. In the free flow case, the flow velocity decreases with the increase in the downstream region length and this will be reflected in the flow velocity because of the friction losses. Here, the friction losses occur between the water flow and the flume-wetted perimeter. In addition to that, the water depth decreases with the increase in the length of the downstream region. This will be reflected on the relationship regardless of the flow cross-sectional area which crosses the gate A_g . In the submerged flow case, the obstacle contributes to the increase of the water depth in the downstream region, but the energy losses increase and this leads to the decrease in the flow velocity regardless of the flow cross-sectional area which crosses the gate A_g . It is noticeable that any sudden change in the flow velocity and the flow depth will be reflected directly on the Reynolds number. The maximum and minimum Reynolds numbers occur in the submerged flow condition while the values of the Reynolds numbers in the free flow condition are distributed between the maximum and minimum values, respectively. Figure 3d illustrates the change of upstream Froude number with (A_g/BH) . The figure introduces a comparative study between the free flow condition and the submerged flow condition. Actually, there is no theoretical equation or empirical equation found between upstream Froude number and (A_g/BH) ; therefore, we can consider both parameters as being independent. Figure 3d reveals a considerable pattern and this occurs owing to the difference in the hydraulic variables which dominate the Froude number and the ratio (A_g/BH) . Here, the Froude number relies on upstream flow velocity and upstream flow depth while the ratio (A_g/BH) relies on upstream discharge and upstream flow velocity. Therefore, the common hydraulic variable, which dominates the relationship, is in fact the upstream flow velocity.

Figure 4a shows the variation of the actual discharge relationship with (y/H) . The figure illustrates a comparative study between the free flow condition and the submerged flow condition. For both flow conditions, the actual discharge values decrease with the increase in (y/H) values. This occurs owing to the confinement of the flow behind the distance (y) and this will be reflected on the actual discharge. This figure shows the influence of the vertical distance between the weir and gate (y) on actual discharge.

Figure 4b illustrates the variation of the discharge coefficient relationship with (y/H) . The figure illustrates a comparative study between the free flow condition and the submerged flow condition. The discharge coefficient values are increased with the increase in (y/H) values. Many hydraulic variables dominate this relationship and these variables are water depth above the weir crest, water depth at gate opening, upstream water depth and downstream water depth.

Figure 5a illustrates the interesting relationship found between the actual discharge and the Reynolds number. The figure illustrates a comparative study between the free flow condition and the submerged flow condition. The figure also shows a linear trend between the actual discharge and the Reynolds number for both flow conditions. Here, the actual discharge and Reynolds number depend on flow velocity. Also, the actual discharge and the Reynolds number have a direct proportion with the flow velocity; therefore, the similarity between both conditions of the flow will occur regardless of the presence of the obstacles in the submerged flow condition.

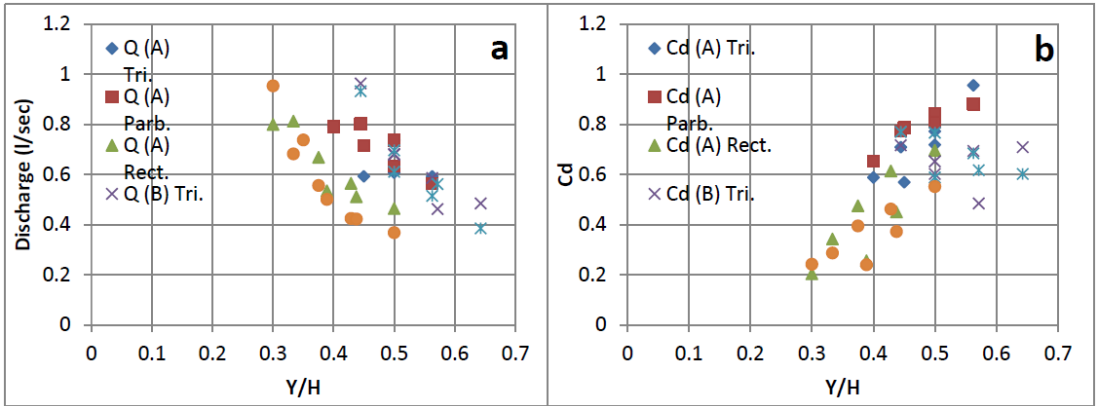


Figure 4 - Distance between weir and gate ratio with (a) Variation of Measured Discharge, (b) Variation of Measured Discharge

Figure 5b illustrates another interesting relationship found between the discharge coefficient and the Reynolds number. The figure illustrates a comparative study between the free flow condition and the submerged flow condition. The figure shows a randomly non-uniform pattern between the discharge coefficient and the Reynolds number. This occurs owing to the interaction between the overflow discharge from the weir and the underflow discharge from the gate, Also, the effect of the downstream obstacle has a significant role in the submerged flow condition.

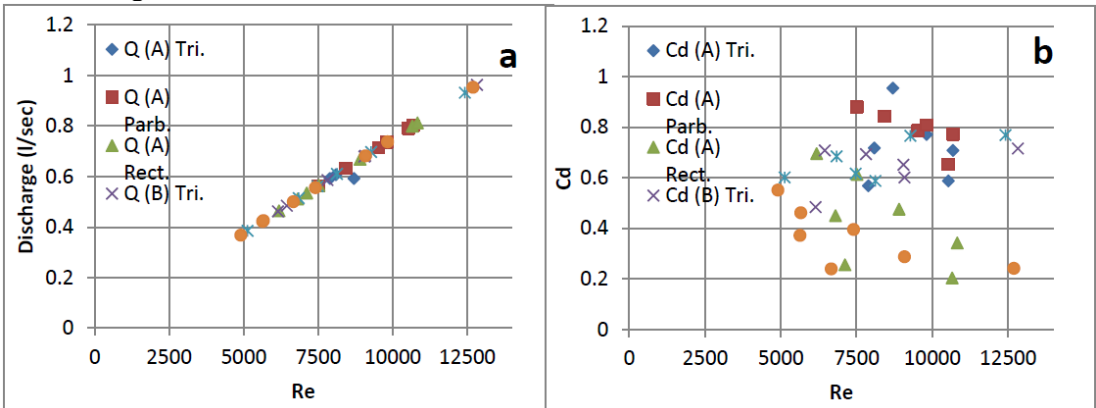


Figure 5 - Reynolds Number with (a) Variation of Measured Discharge, (b) Variation of Discharge Coefficient

Figure 6 shows the relationship between the discharge coefficient and flow velocity for the free flow and the submerged flow. A complex relationship is found due to the interaction between the weir flow velocity and the gate flow velocity. In the condition of submerged flow, the flow velocity values are less than the values of the flow velocity in the condition of free flow.

The flow velocity in the free flow condition has a range between fivefold to six fold the flow velocity in the submerged flow condition. Based on equations (7, 15 and 22), the discharge coefficient of composite structure has an inverse relationship with the flow velocity. So, any increase or decrease in the flow velocity will be reflected in the values of the discharge coefficient. Moreover, the presence of the obstacles at the flume bed will be shared in the complexity of the relationship between the discharge coefficient and the flow velocity as compared with the flume bed without the obstacles.

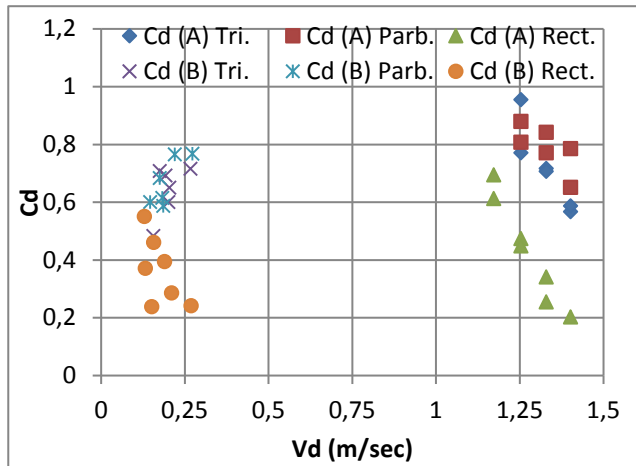


Figure 6 - Variation of Discharge Coefficient with downstream Velocity

Figure 7 shows the relationship between the discharge coefficient and the average water depth in the downstream region for free flow and submerged flow. From this figure, it is obvious that the relationship is complex. Actually, there is no theoretical equation or empirical equation between the discharge coefficient and the water depth in downstream, therefore, these parameters can be considered independent. It is also clear from the figure that when the water depth in the downstream region increases, the discharge coefficient will decrease too and this will occur in the submerged flow condition while the reverse occurs in the free flow condition. Any fluctuation in the results found is attributed to the interaction between weir flow velocity and gate flow velocity.

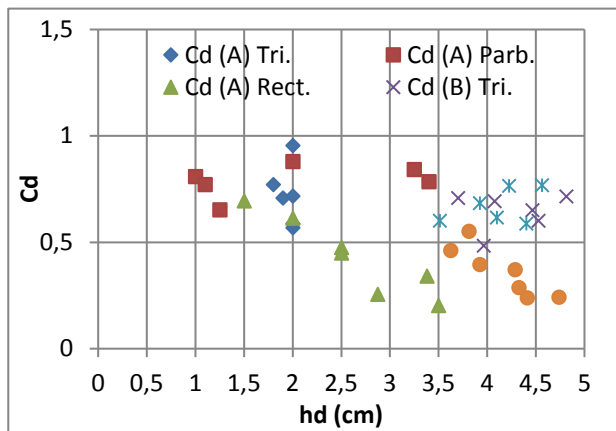


Figure 7 - Variation of Discharge Coefficient with downstream water depth

Figure 8 illustrates the change of downstream Froude number with (A_g/BH) . It also illustrates a comparative study between the free flow condition and the submerged flow condition. Actually, there is no theoretical equation or empirical equation found between downstream Froude number and (A_g/BH) , therefore, we can consider both parameters as independent ones. In the free flow condition, the Froude number values are higher with the increase in (A_g/BH) values. The values of the Froude number in the submerged flow condition are less than the values of the Froude number in the free flow condition. Really, the Froude number depends on the flow velocity and the flow depth.

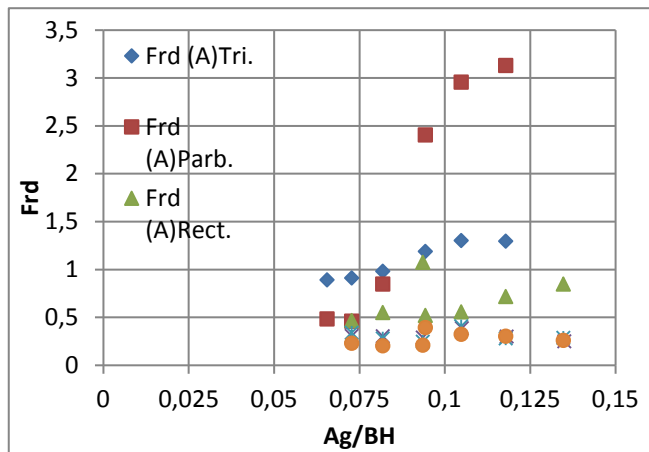


Figure 8 - Variation of downstream Froude Number with Area of Gate Ratio

The existence of obstacles in the submerged flow condition leads to an increase in the water depth and decrease in Froude number while the reverse occurs in the free flow condition. This inferment deals with water depth regardless of flow velocity and despite that, both of them have significant impact on the Froude number.

The experimental work concentrated on increasing the depth of water in the downstream region by using obstacles of different sizes and shapes. The authors make tables in order to show the water depths in downstream; these tables include location and depth. In addition, these tables give the position of maximum and minimum water depth.

Table 2 - Downstream Water Surface for Energy Dissipater Type (W)

Model No.	10 cm	20 cm	30 cm	40 cm	50 cm	60 cm	70 cm	80 cm	$h_d(\text{avg.})$ W.O
1	5.3	5.5	5.5	5.0	4.2	4.0	4.0	4.0	2.0
2	5.0	5.0	5.0	4.7	4.0	4.0	3.7	3.7	1.9
3	4.8	4.8	4.5	4.3	3.5	3.5	3.3	3.0	1.8
4	5.1	5.3	5.3	4.8	4.3	4.3	3.8	3.6	2.0
5	4.7	4.8	4.8	4.3	3.8	3.8	3.6	3.4	2.0
6	4.3	4.4	4.4	3.9	3.5	3.5	3.2	3.0	2.0
7	5.5	5.8	5.8	5.4	4.5	4.5	4.3	4.0	1.3
8	5.0	5.0	4.8	4.5	4.0	4.0	3.8	3.6	1.1
9	4.7	4.7	4.3	4.3	3.6	3.6	3.4	3.4	1.0
10	5.0	5.0	5.0	4.7	4.2	4.0	3.6	3.2	3.4
11	4.6	4.6	4.4	4.3	3.5	3.3	3.0	3.0	3.3
12	4.3	4.3	4.2	3.8	3.2	3.2	3.0	2.8	2.0
13	5.4	5.5	5.4	5.2	4.3	4.3	4.2	3.8	3.5
14	4.7	5.1	5.0	4.7	4.2	4.1	3.7	3.7	3.4
15	4.6	4.8	4.6	4.3	3.7	3.8	3.3	3.0	2.5
16	4.2	4.3	4.3	4.0	3.3	3.4	3.0	2.8	2.0
17	4.5	4.5	4.1	4.0	3.4	3.4	3.1	3.0	2.9
18	4.3	4.3	3.8	3.8	3.1	3.1	2.7	2.7	2.5
19	4.0	4.0	3.5	3.5	2.8	2.8	2.5	2.5	1.5
20	5.0	5.2	5.0	4.8	4.5	4.3	4.0	4.0	2.8
Minimum	4.0	4.0	3.5	3.5	2.8	2.8	2.5	2.5	1.0
Maximum	5.5	5.8	5.8	5.4	4.5	4.5	4.3	4.0	3.5

Here, High competition occurs in maximum and minimum water depth and some of these depth values are close.

So satisfactory and reasonable water depths are obtained with using the obstacles in the downstream region and as compared without using these obstacles. Tables 2, 3, 4 and 5 show all the details of water depth and location.

Table 3 - Downstream Water Surface For Energy Dissipater Type (C)

Model No.	10 cm	20 cm	30 cm	40 cm	50 cm	60 cm	70 cm	80 cm	h _d (avg.) W.O
1	5.5	5.8	5.8	5.0	4.3	4.3	4.3	4.3	2.0
2	5.1	5.3	5.3	4.8	3.9	4.0	3.7	3.7	1.9
3	4.8	4.8	4.5	4.3	3.4	3.6	3.3	3.0	1.8
4	5.0	5.3	5.3	4.8	4.0	4.0	3.7	3.4	2.0
5	4.8	4.8	4.6	4.4	3.6	3.8	3.7	3.3	2.0
6	4.4	4.4	4.2	4.0	3.2	3.4	3.3	3.0	2.0
7	5.5	5.7	5.7	5.2	4.3	4.4	4.0	4.0	1.3
8	5.0	4.8	4.5	4.0	3.8	3.8	3.8	3.6	1.1
9	4.7	4.5	4.2	3.6	3.5	3.3	3.3	3.1	1.0
10	4.8	5.0	4.8	4.5	4.0	3.8	3.6	3.6	3.4
11	4.7	4.7	4.3	4.3	3.4	3.5	3.3	3.0	3.3
12	4.3	4.3	4.0	3.8	3.2	3.0	2.7	2.5	2.0
13	5.2	5.5	5.2	5.2	4.2	4.2	4.2	4.0	3.5
14	4.6	5.0	5.0	4.8	4.3	4.0	3.8	3.6	3.4
15	4.6	4.7	4.5	4.2	3.8	3.9	3.3	3.0	2.5
16	4.2	4.3	4.2	4.1	3.3	3.2	3.0	2.8	2.0
17	4.8	5.0	5.0	4.8	4.0	4.1	3.9	3.7	2.9
18	4.5	4.8	4.8	4.5	3.6	3.7	3.5	3.4	2.5
19	4.5	4.5	4.5	4.3	3.3	3.3	3.1	2.9	1.5
20	5.0	5.2	5.2	5.0	4.2	4.3	4.1	3.9	2.8
Minimum	4.2	4.3	4.0	3.6	3.2	3.0	2.7	2.5	1.0
Maximum	5.5	5.8	5.8	5.2	4.3	4.4	4.3	4.3	3.5

Table 4 - Minimum Water Surface Profile for Different Energy Dissipater Type (EDT)

E.D.T	Model No.	10 cm	20 cm	30 cm	40 cm	50 cm	60 cm	70 cm	80 cm
Y	12	4.2	4.2	4.0	3.7	3.3	3.1	2.9	2.7
H	12	4.3	4.3	4.0	3.8	3.3	3.2	3.0	2.8
C	12	4.3	4.3	4.0	3.8	3.2	3.0	2.7	2.5
T	19	4.1	4.1	4.0	3.5	3.0	3.0	2.7	2.7
W	19	4.0	4.0	3.5	3.5	2.8	2.8	2.5	2.5
L	19	4.0	3.8	3.8	3.5	3.1	2.8	2.8	2.3
Z	19	4.0	4.0	3.7	3.7	3.7	2.9	2.8	2.6
I	19	4.0	4.0	3.8	3.5	2.9	2.9	2.7	2.7
N	19	4.0	4.0	3.7	3.6	3.3	3.0	2.7	2.7
E	19	4.1	3.8	3.6	3.3	3.1	2.8	2.8	2.5
X	19	4.1	4.0	4.0	3.6	3.2	3.1	2.8	2.6
U	19	4.1	4.1	3.8	3.8	3.2	3.2	3.0	2.8
	Minimum	4.0	3.8	3.5	3.3	2.8	2.8	2.5	2.3
	Maximum	4.3	4.3	4.0	3.8	3.7	3.2	3.0	2.8

Table 5 - Maximum Water Surface Profile for Different Energy Dissipater Type (EDT)

E.D.T	Model No.	10 cm	20 cm	30 cm	40 cm	50 cm	60 cm	70 cm	80 cm
Y	1	5.5	5.5	5.5	5.0	4.5	4.5	4.0	4.0
H	1	5.5	5.8	5.5	5.3	4.5	4.5	4.3	4.3
C	1	5.5	5.8	5.8	5.0	4.3	4.3	4.3	4.3
T	1	5.3	5.7	5.7	5.0	4.7	4.5	4.3	4.3
W	7	5.5	5.8	5.8	5.4	4.5	4.5	4.3	4.0
L	7	5.3	5.5	5.5	5.3	4.5	4.5	4.3	4.0
Z	7	5.5	5.8	5.8	5.3	4.5	4.3	4.0	4.0
I	7	5.5	5.8	5.8	5.3	4.5	4.5	4.7	4.2
N	7	5.3	5.5	5.5	5.3	4.8	4.5	4.3	4.1
E	7	5.5	5.8	5.8	5.3	4.5	4.5	4.3	4.0
X	7	5.3	5.7	5.7	5.4	4.8	4.6	4.3	4.2
U	1	5.4	5.7	5.7	5.3	4.5	4.5	4.0	4.0
	Minimum	5.3	5.5	5.5	5.0	4.3	4.3	4.0	4.0
	Maximum	5.5	5.8	5.8	5.4	4.8	4.5	4.7	4.3

5. CONCLUSIONS

The objective of this research is to investigate the impact of an obstacle in the downstream region compared with the state of not using it. The following important points have been arrived at by the researchers for this research.

- 1- The main objective of using the obstacles refers to increasing the rising of water depth in the downstream region.
- 2- the difference between free flow and submerged flow appears clearly in the trend between the different variables (hydraulic variable and geometrical variable)
- 3- The cross-sectional area of flow that crosses the gate has a major effect on actual discharge, discharge coefficient, Reynolds number, upstream Froude number and downstream Froude number regardless of the presence of obstacles at downstream region.
- 4- The distance between weir and gate has a noticeable impact on the actual discharge.
- 5- There is a linear trend between the actual discharge and Reynolds number regardless of the presence of obstacles in the downstream region.
- 6- There exists a random pattern between the discharge coefficient and Reynolds number.
- 7- There is a complex pattern between discharge coefficient and flow velocity.
- 8- Both discharge coefficients of composite structure and water depth downstream are considered independent parameters.
- 9- The shape and size of obstacle has direct impact on water depth at downstream region.
- 10- The fluctuation in the results was found owing to the interaction between the overflow velocity and the underflow velocity.
- 11- The selection of a suitable obstacle is based on maximum and minimum water depth elevation and location.

REFERENCES

- [1] T. Tingsanchali, and S. Maheswaran, 2-D depth-averaged flow computation near groyne, *Journal of Hydraulic Engineering* **16**, 71–86, 1990.
- [2] M. Michiue, and O. Hinokidani, Calculation of 2-dimensional bed evolution around spur-dike, *Annu. Journal of Hydraulic Engineering, Japan Soc. Civ. Eng.*, **36**, 61–66, 1992.
- [3] Y. Jia and S. S. Wang, 3D numerical simulation of flow near a spur dike, *Proceedings of 1st International Conference on Hydro-Science and Engineering*, Washington, D.C., 2150–2156, 1993.

- [4] N. Muneta, and Y. Shimizu, Numerical model with spur-dike considering the vertical velocity distribution, *Proc., Japan Society of Civil Engineers Conf.*, Tokyo **497**, 31–39, 1994.
- [5] R. Mayerle, F. M. Toro, and S. S. Wang, Verification of a three dimensional numerical model simulation of the flow in the vicinity of spur dikes, *Journal of Hydraulic Research* **33**, 243–256, 1995.
- [6] S. Ouillon and D. Dartus, Three-dimensional computation of flow around groyne, *Journal of Hydraulic Engineering* **123**, 962–970, 1997.
- [7] F-Y. Chen, and S. Ikeda, Horizontal separation flows in shallow open channels with spur dikes, *Journal of Hydrosience and Hydraulic Engineering* **15**, 15– 30, 1997.
- [8] I. Kimura, and T. Hosoda, 3-D unsteady flow structures around rectangular column in open channels by means of non-linear k- ϵ model, *Proceedings of 1st International Symposium on Turbulence and Shear Flow Phenomena*, Santa Barbara, California, USA, 1001–1006, 1999.
- [9] A. A. Alhamid, Effective roughness on horizontal rectangular stilling basins, *Trans. Ecol. Environ.*, **8**, 39–46, 1994.
- [10] Y. Jia, S. Scott, Y. Xu, S. Huang, S. Y. Wang, Three-dimensional numerical simulation and analysis of flows around a submerged weir in a channel bendway, *J Hydraul Eng* 2005: **131**(8): 682-93
- [11] N. Nagata, T. Hosoda, T. Nakata, Y. Muramoto, Three-dimensional numerical model for flow and bed deformation around river hydraulic structures, *J Hydraul Eng* 2005: **131**(12): 1074-87.
- [12] R. M. Qasim, I. A. Abdulhussein, K. Al-Asadi, The effect of barrier on the hydraulic response of composite weir-gate structure, *Archives of civil engineering*, Vol. **LXVI**, issue 4, 2020.
- [13] R. M. Qasim, I. A. ABDULHUSSEIN, A. A. MOHAMMED, Q. A. MAATOOQ, The effect of the obstacle on the hydraulic response of the composite hydraulic structure, *INCAS BULLETIN*, Volume **12**, Issue 3, pp. 159 – 172, 2020, <https://doi.org/10.13111/2066-8201.2020.12.3.13>
- [14] V. L. Streeter and E. B. Wylie (1983), *Fluid Mechanics*, First SI Metric Edition, 1983.
- [15] M. G. Bos, *Discharge Measurement Structures*, 3rd Edition International Institute for Land Reclamation and Improvement/ Wageningen, The Netherlands, 1989.
- [16] A.-A. M. Negm, A. M. AL- Brahim, A. A. Alhamid, Combined-Free Flow Over Weirs and Below Gates, *J. Hydraul. Res.* **40**, 1–7, 2002.
- [17] R. W. Fox, T. McDonald, *Introduction to Fluid Mechanics*, 4th ed., John Wiley & Sons, New Delhi, 1994.
- [18] R. M. Qasim, I. A. Abdulhussein, M. A. Hameed, and Q. A. Maatooq, Experimental study of coupled parabolic weir over Flow and gate under flow rate, *Journal of Information Engineering & Application*, **8**, 34–42, 2018.